Optical and Quantum Electronics (2026) 58:219
https://doi.org/10.1007/s11082-026-08794-4

Mid-infrared radiation generation in air by four-wave mixing of femtosecond laser pulses

Virgilijus Vaičaitis[1] · Mateusz Rebarz[2] · Shirly Espinoza[2] · Ona Balachninaitė[1]

Received: 5 February 2026 / Accepted: 25 March 2026 / Published online: 15 April 2026
© The Author(s) 2026

Abstract
Tunable mid-infrared radiation in the range of 2.06–12 μm was generated in air via loosely focused two-color femtosecond laser pulses. The emission spectra and beam profiles confirm its origin as four-wave difference-frequency mixing in a low-density air plasma filament. Near phase-matching due to low air dispersion opens possibilities for efficient energy conversion at high powers.

Keywords Four-wave mixing · Mid-infrared radiation · Nonlinear optics · Femtosecond lasers · Air plasma

1 Introduction

Sources of coherent mid-infrared (mid-IR) radiation, which, according to the international standard ISO 20473:2007 covers the wavelengths from 3 μm to 50 μm are of great interest for a wide range of scientific and technological applications, such as ultrafast IR spectroscopy (Calabrese et al. 2012), biomedicine (Jean and Bende 2003), infrared imaging (Israelsen et al. 2019), laser material processing (Werner et al. 2019), etc. In addition, due to the fact that the ponderomotive potential scales with the square of the laser wavelength, the long wavelength pump pulses are preferable for various strong-field physics and attoscience

✉ Shirly Espinoza
shirly.espinoza@eli-beams.eu

Virgilijus Vaičaitis
virgilijus.vaicaitis@ff.vu.lt

Mateusz Rebarz
mateusz.rebarz@eli-beams.eu

Ona Balachninaitė
ona.balachninaite@ff.vu.lt

[1] Laser Research Center, Vilnius University, Saulėtekio 10, Vilnius LT-10223, Lithuania

[2] ELI Beamlines Facility, The Extreme Light Infrastructure ERIC, Za Radnicí 835, Dolní Břežany 25241, Czech Republic

applications, including the high-order harmonic and broadband terahertz (THz) radiation generation from laser-created plasmas (Brabec and Krausz 2000; Jang et al. 2019; Clerici et al. 2013).

Though there are many methods of coherent mid-IR radiation generation, each of them suffers from some inherent drawbacks. Thus, the lasers based on rare-earth doped fluoride fibers (Ma et al. 2019) and transition-metal doped chalcogenides (Mirov et al. 2018) as well as mid-IR supercontinuum generators in fibers and waveguides (Yu et al. 2013; Liu et al. 2014) can not provide high output powers, while the quantum cascaded lasers (Yao et al. 2012), in addition, have very limited wavelength tunability. Therefore, to obtain powerful, ultrashort mid-infrared radiation pulses, an optical parametric amplifier (OPA) combined with difference-frequency generation in nonlinear crystals can be used. These systems can provide moderately high output powers and peak intensities (Wilson et al. 2019) in very broad wavelength tuning ranges (Steinle et al. 2016). When extremely high powers and intensities are required, optical parametric chirped pulse amplification (OPCPA) systems must be used (Dubietis and Matijošius 2023). However, powerful OPCPA systems have low wavelength tunability. Additionally, almost all of the aforementioned methods require materials (e.g., nonlinear crystals or active laser media) that are transparent in the spectral ranges of both the pump and the emitted mid-IR radiation. The choice of materials is very limited, since the wavelength difference between the pump and mid-IR pulses is usually quite large. Therefore, these materials are often expensive or lack the necessary properties such as high optical nonlinearity and good thermal conductivity. Conversely, common, readily available gases, including ambient air, have broad transparency regions in the ultraviolet (UV), visible, and infrared (IR) spectral ranges, which can be used for nonlinear optical frequency conversion. Note, however, that in gaseous media the lowest order optical nonlinearity is the third-order one, which is by a few orders of magnitude lower than the second-order nonlinearity present in non-centrosymmetric crystals (Boyd 2003). Therefore, in general, efficient frequency conversion in gases requires a much higher pump intensity than that required for nonlinear interactions in crystals. However, note that in resonant gaseous media, the frequency conversion efficiency could be comparably high even in the case of low pump powers (Gaižauskas et al. 2013; Lukin et al. 2000).

Nevertheless, since the advent of picosecond and femtosecond lasers, gaseous media have been widely used for various types of radiation generation. Thus, the high harmonic and attosecond pulse generation in gas jets, as well as terahertz (THz) generation in air, have become routine processes used in many laboratories (Li et al. 2020; Kim et al. 2008; Vaičaitis et al. 2018). Other nonlinear processes, such as four-wave mixing (Vaičaitis 2000; Théberge et al. 2006), third harmonic generation (Tamulienė et al. 2020; Aközbek et al. 2002), and supercontinuum generation (Vaičaitis et al. 2018), are still being actively investigated. This includes mid-infrared radiation generation in air by femtosecond laser pulses, when the fundamental and second harmonics (FH and SH respectively) are mixed together to produce the broadband mid-IR radiation (Fuji and Suzuki 2007). Though this approach is very simple and efficient, to the best of our knowledge, narrowband and widely tunable mid-IR radiation generation has not yet been demonstrated using this method. Therefore, in this paper, we present a proof-of-principle experiment that demonstrates the generation of tunable mid-infrared radiation through the four-wave difference-frequency mixing of femtosecond laser pulses in air. In contrast to the experiments referenced above, we mixed the fundamental radiation (FW) of a femtosecond Ti:sapphire laser and the widely tunable

signal wave of an optical parametric amplifier (OPA) instead of the FH and SH pulses. This allowed us to generate mid-infrared radiation in the 2.06–12 μm range.

2 Experimental

The experiment was performed with the laser system located at the ELI Beamlines facility (Dolní Břežany, Czech Republic). The experimental setup is shown in Fig. 1. The primary source was an amplified Ti:Sapphire femtosecond laser with its fundamental mode at 800 nm and a repetition rate of 1 kHz (Coherent Astrella, 35 fs, max. 6 mJ). Part of the primary beam ($\sim$ 1.5 mJ) was used to generate a signal wave (SW, tunable from 1.1 to 1.6 μm) in an optical parametric amplifier (TOPAS Prime, Light Conversion). A dichroic mirror (R$>$ 99% at 800 nm, T$>$ 90% at 1100–2600 nm, Altechna) combined another part of the fundamental laser beam (FW, $\sim$ 3 mJ) with the SW beam to make them collinear.

The FW and SW beams were focused with separate lenses (L1 and L2) of different focal lengths (96 cm and 75 cm for the FW and SW beams, respectively). The initial beam diameters were 13.5 mm (FW) and 3.5 mm (SW) at the $1/e^2$ intensity level. Timing of the FW and SW pulses was controlled by an optical delay line (DL), composed of a retroreflector (Omniwave 25-1 G, PLX) installed on a motorized linear stage (IMS-LM-S, Newport), while the spatial overlap of the beam waists along the optical axis was adjusted by varying the positions of the lenses L1 and L2. During most measurements, the SW power was kept maximal (constant at about 110 mW), while the FW power was varied within a wide range (from 22 mW to 3.1 W) using an attenuator composed of a half-wave plate and a wire-grid polarizer.

The pump and any residual radiations were blocked by an IR long pass filter (OD$>$ 3 at 200–2400 nm, T$>$ 85% at 2520–4800 nm, Edmund Optics), while the generated IR radiation was focused by an off-axis parabolic mirror (RFL = 6 inch) on the slit of the Czerny–Turner spectrograph (SP–2150, Princeton Instruments) with IR grating (75 g/mm, 4.65 μ m blazed). Dispersed light (or 0th order reflection) was detected by liquid nitrogen cooled mercury–cadmium–telluride detector (2DMCT Phasetech, 128 $\times$ 128 pixels, 1 kHz read-

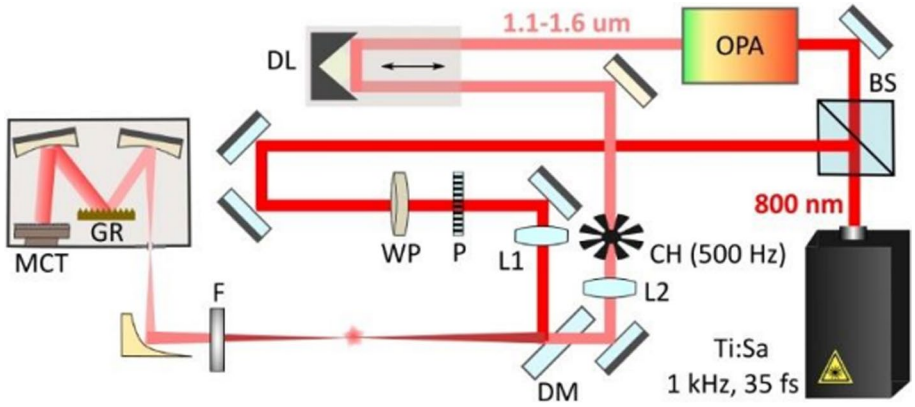

Fig. 1 Experimental setup. BS – beam splitter, CH – chopper, DL – delay line, DM – dichroic mirror, F – IR long-pass filter, GR – IR grating, L1, L2 – quartz lenses, MCT – HgCdTe detector, OPA – optical parametric amplifier, P – polarizer, WP – half-wave plate

out rate). An optical chopper was inserted into the beam path to interrupt the FW beam at 500 Hz repetition rate. It enabled to reduce noise and to register the background-free radiation signal. Polarizations of the FW and SW beams were controlled with the help of the half-wave plate inserted into the FW beam path.

3 Results

When the SW and FW pulses were combined spatially and temporally, clearly visible conical radiation emerged from the interaction zone (Fig. 2a). We identified this phenomenon as four-wave mixing, which occurs when two FW photons and one SW photon combine to produce a new photon with a different frequency.

$$\omega_{\mathrm{vis}} = 2\omega_{\mathrm{FW}} - \omega_{\mathrm{SW}}, \tag{1}$$

where ω_{vis}, ω_{FW} and ω_{SW} are the frequencies of the visible, FW and SW radiations, respectively (Fig. 3a). Note that this type of interaction has already been analyzed in detail (Théberge et al. 2006), therefore in this work we used it for the alignment of SW and FW beams.

Note that another type of four-wave mixing is also possible in air, when two SW photons and one FW photon are mixed together to produce the one in the mid-IR spectral range (Fig. 3b). The frequency of this radiation $\omega_{\text{mid-IR}}$ is defined by the relation:

$$\omega_{\text{mid-IR}} = 2\omega_{\mathrm{SW}} - \omega_{\mathrm{FW}}. \tag{2}$$

Since both processes are the result of a common action of the FW and SW pulses and the visible and mid-IR radiations are generated only when both pump pulses are overlapped in time, first we have registered dependencies of the mid-IR radiation spectra as a function of the delay between the FW and SW pulses for various FW pulse energies. The results are presented in Fig. 4.

As one can see, the central wavelength was about 3.3 μm for the SW wavelength of 1.29 μm, independently of the FW pulse energy. However, the spectral width of the gener-

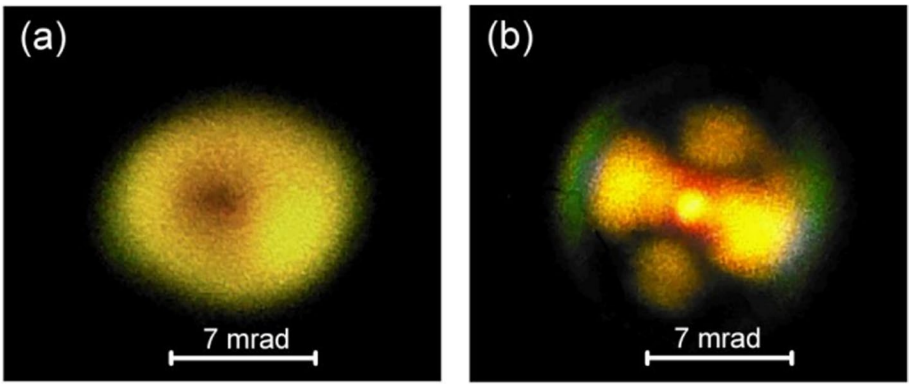

Fig. 2 Typical angular distributions of the visible emission generated in air at SW wavelength of 1.29 μm and FW pulse energies of 0.1 mJ (**a**) and 1 mJ (**b**)

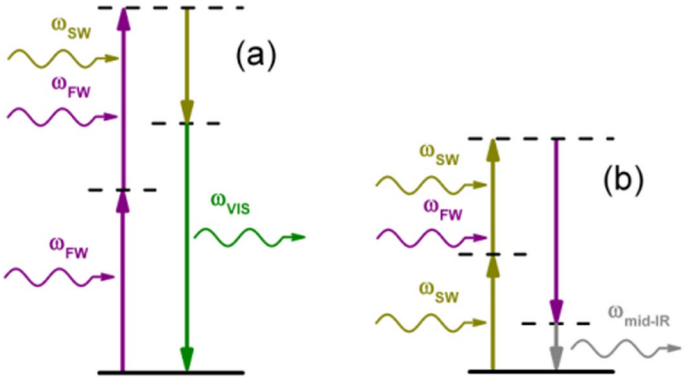

Fig. 3 Schematic diagrams of the four-wave mixing producing the visible (**a**) and mid-IR (**b**) radiations. ω_{SW}, ω_{FW}, ω_{VIS} and $\omega_{\mathrm{mid\text{-}IR}}$ are the frequencies of SW, FW and generated visible and mid-IR radiations, respectively

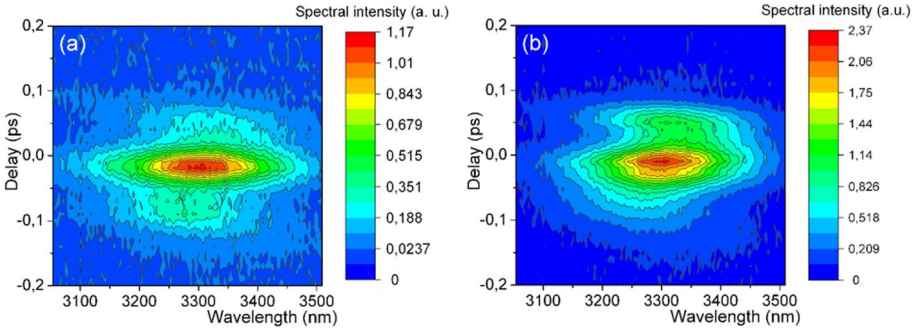

Fig. 4 Spectra of the mid-IR radiation as a function of delay between the FW and SW pulses for the FW pulse energy of 0.5 mJ (**a**) and 2 mJ (**b**). SW wavelength was 1.29 μm

ated mid-IR radiation depended slightly on the pump power. Specifically, it decreased from approximately 215 to 200 nm (at the full width at half maximum (FWHM) level) as the FW pulse energy increased from 0.5 to 2 mJ. The time dependence of the signal was also almost independent of the pump power and consisted of a single peak of approximately 46 fs at the FWHM level. This corresponds to the third-order intensity cross-correlation of two pump pulses (one FW pulse of 35 fs and one SW pulse of 40 fs). However, at high FW pulse energies (above 1 mJ), a weak secondary peak appeared, separated by about 80 fs from the main peak (Fig. 4b). We believe that this peak results from temporal splitting of the FW pulse during propagation in air, a phenomenon that has been observed under similar experimental conditions (Gaižauskas et al. 2016). Note that this feature was more pronounced when for the pump focusing the shorter focal length lenses (30 or 50 cm) were used. Note also that the SW pulse was less susceptible to temporal broadening and splitting because its peak intensity was much lower than that of the FW pulse.

The wavelength dependence of the generated mid-infrared radiation corresponds well to Equation (2). Thus, when the SW wavelength varied from 1.15 to 1.5 μm, the wavelength of the mid-IR radiation increased from 2.06 to 12 μm (Fig. 5a). The maximum emission power

was registered when the SW wavelength was set to 1.29 μm. However, the mid-IR power decreased sharply when the SW wavelength was detuned to shorter or longer values. This phenomenon can be partially explained by the fact that the energy of the SW pulse generated by the OPA was maximal at this wavelength, dropping by a factor of three or even more at the extremes of its tuning range.

Under the undepleted pump and slowly varying envelope approximations of the four-wave mixing, the evolution of the mid-IR radiation field $A_{\text{mid-IR}}$ with frequency ω_{IR} along the interaction length z can be described by the following equation (Penzkofer and Lehmeier 1993):

$$\frac{dA_{\text{mid-IR}}}{dz} = -i\frac{3\omega_{\text{IR}}}{2n_{\text{IR}}c}\chi^{(3)}A_{\text{SW}}^2 A_{\text{FW}}^* e^{i\Delta kz}, \tag{3}$$

where A_{SW}, A_{FW} and $\Delta k = 2k_{\text{SW}} - k_{\text{FW}} - k_{\text{mid-IR}}$ are the complex amplitudes of the SW and FW fields and wave mismatch, while n_{IR}, c and $\chi^{(3)}$ are the refractive index at ω_{IR}, speed of light in vacuum, and the relevant third-order nonlinear susceptibility component of air, respectively.

The dependencies of mid-infrared radiation power on FW and SW pulse energies presented in Fig. 6 are consistent with predictions following from Eq. (3). Thus, the dependence of the mid-IR pulse energy on the SW pulse energy was nearly perfectly quadratic (see the red dashed line in Fig. 6a). Also, as expected, at low FW pulse energies (below 1 mJ), the mid-IR pulse energy increased nearly linearly with the FW pulse energy. Above this level, however, the linear dependence began to saturate, and for FW pulse energies above 1.25 mJ, the mid-IR pulse energy remained nearly constant, oscillating around 90 nJ. We believe that this abrupt saturation of the mid-IR power is caused by the onset of multiple FW beam filamentation and rapid plasma density growth in the interaction zone. This results in the absorption of the generated mid-IR signal (Vaičaitis et al. 2023) and modification of the FWM phase-matching conditions, which can be confirmed by the fact that, at high FWM

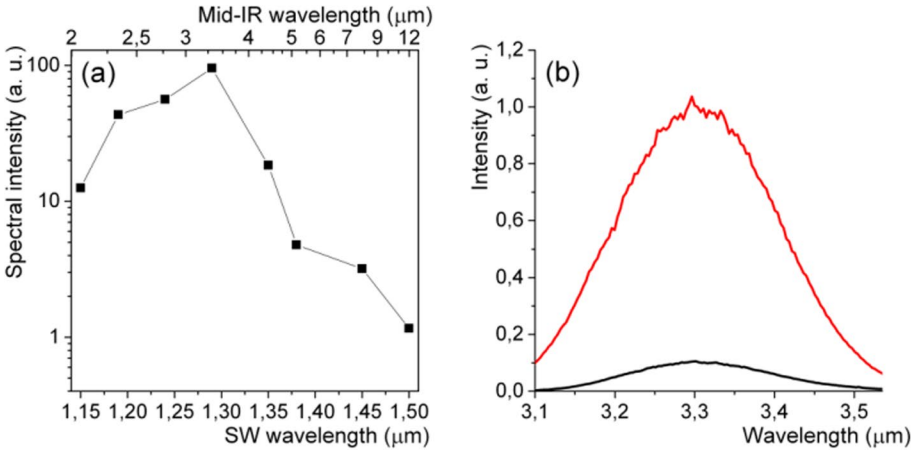

Fig. 5 Wavelength and power dependence of generated mid-IR radiation on SW wavelength at maximal FW and SW pulse energies (**a**) and typical spectra of the mid-IR radiation (**b**), registered with orthogonal and parallel FW and SW polarizations (black and red lines, respectively) for the SW wavelength of 1.29 μm

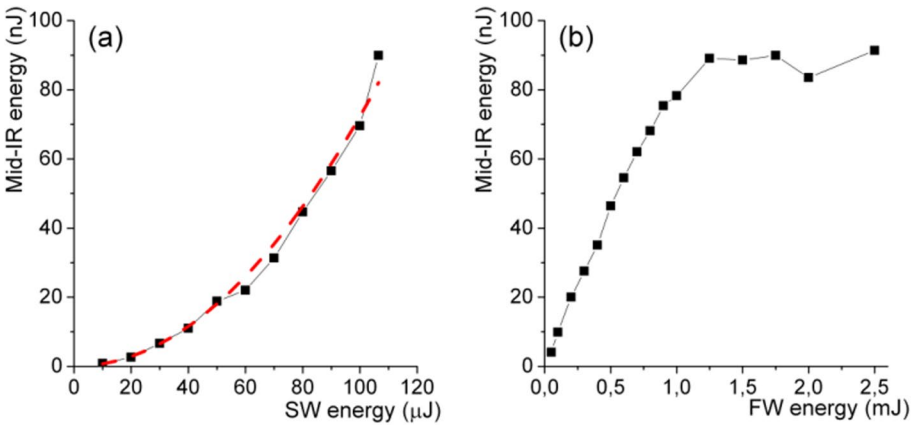

Fig. 6 Mid-IR radiation pulse energies as a function of FW (**a**) and SW (**b**) pulse energies for SW wavelength of 1.29 μm, with a fixed FW pulse energy of 1 mJ (**a**) and SW pulse energy of approximately 0.1 mJ (**b**). The red dashed line in (**a**) represents a quadratic fit of the experimental data

pulse energies, the visible conical radiation–also resulting from FWM–became crest-shaped (compare Fig. 2a and b).

Note that the efficiency of mid-IR radiation generation was significantly higher (by a factor of almost 10) for parallel SW and FW polarizations than for orthogonal ones (see Fig. 5b). This also follows from Equation (3), since in the case of parallel polarizations the FWM is governed by the third-order susceptibility component, $\chi^{(3)}_{xxxx} = \chi^{(3)}_{yyyy}$, which is three times larger than the component involved in mid-IR radiation generation with orthogonal pump polarizations (Dietze et al. 2009).

The spatial characteristics of the SW beam were examined using a moving knife positioned just before the collimating parabolic mirror (see Fig. 1). Figure 7a shows the power dependence of the mid-infrared radiation on the knife-edge position. As expected, when the knife is not blocking the beam (at coordinates less than $-5\,\mathrm{mm}$), the transmitted mid-IR power is maximal. It remains at this level until the knife edge begins to obstruct the beam and fully blocks it (at coordinates greater than $5\,\mathrm{mm}$).

The obtained experimental data were fitted using a sigmoid function (Khosrofian and Garetz 1983):

$$I_{\mathrm{tot}}(x) = \frac{A}{2}\left[1 - \mathrm{erf}\left(\frac{\sqrt{2}(x - x_0)}{w}\right)\right], \tag{4}$$

where I_{tot} is the total beam power, and w is the Gaussian beam radius at the $1/e^2$ level. The beam diameters were found to be 10.8, 11.1, and 9 mm for FW pulse energies of 0.1, 1, and 2.5 mJ, respectively. Considering that the knife was positioned about 94 cm from the plasma filament's center, these beam diameters correspond to divergences of less than 10 mrad (11.5, 11.8, and 9.6 mrad for the respective FW pulse energies), indicating that nearly diffraction-limited beams were generated during the experiment. Thus, by comparing these values with the diffraction angle θ of the collimated beam, which is defined by the equation:

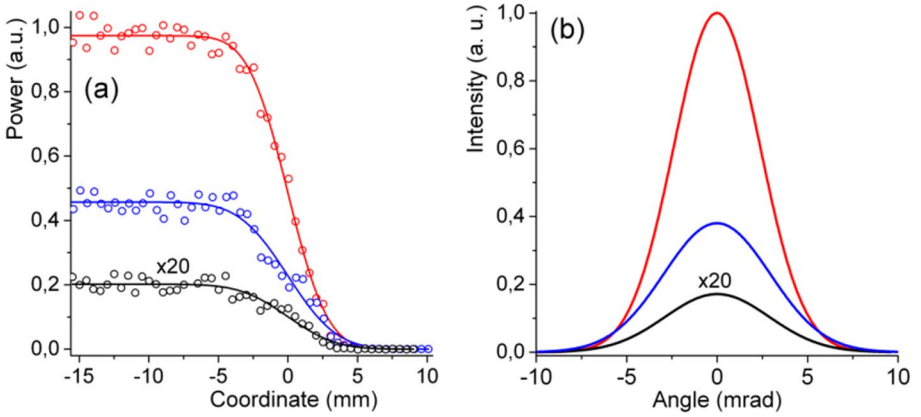

Fig. 7 Power dependencies of the mid-IR radiation as a function of the knife edge position (**a**) and the corresponding angular spectra (**b**) for the FW pulse energies of 0.1, 1 and 2.5 mJ (black, blue and red curves, respectively)

$$\theta = \frac{\lambda_{\mathrm{IR}}}{\pi w}, \tag{5}$$

where λ_{IR} is the wavelength of the mid-IR radiation ($3.3\,\mu\mathrm{m}$), one can find that the divergence corresponds to an initial beam diameter of about $100\,\mu\mathrm{m}$. This agrees qualitatively well with the FW beam diameter in the focal area (the source of the mid-IR radiation) registered under similar experimental conditions (Gaižauskas et al. 2016).

4 Discussion and conclusions

To further analyze the properties of the generated mid-IR radiation, we have estimated the phase mismatch $\Delta\mathrm{K}$ and the coherence length L_c of the four-wave mixing process responsible for its generation. For the phase-matched process described by Eq. (2), the wave vectors of the SW, FW, and the generated mid-IR radiation ($\mathrm{K_{SW}}$, $\mathrm{K_{FW}}$, and $\mathrm{K_{mid\text{-}IR}}$, respectively) are related by the following equation:

$$\mathrm{K_{mid\text{-}IR}} = 2\mathrm{K_{SW}} - \mathrm{K_{FW}}. \tag{6}$$

Then, the phase mismatch $\Delta\mathrm{K}$ can be expressed as:

$$\Delta\mathrm{K} = 2\mathrm{K_{SW}} - \mathrm{K_{FW}} + \mathrm{K_{mid\text{-}IR}} \tag{7}$$

The coherence length L_c (or, more precisely, the coherent buildup length of the interaction) is inversely proportional to the magnitude of the phase mismatch $\Delta\mathrm{K}$:

$$L_c = \frac{2\pi}{|\Delta\mathrm{K}|} \tag{8}$$

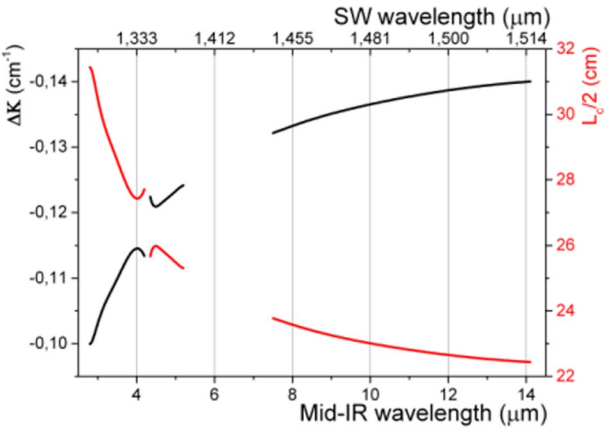

Fig. 8 Dependencies of the four-wave mixing phase mismatch ΔK (black line) and half coherence length $L_c/2$ (red line) on the mid-IR and SW wavelengths

However, in many reports, a twice smaller parameter, $\pi/|\Delta\mathrm{K}|$, is commonly used instead of L_c, since in the first half of the propagation length the nonlinear signal grows faster.

Based on air refractive index data (Ciddor 1996; Mathar 2007) and without considering plasma influence, we have plotted both parameters (ΔK and $L_c/2$) as functions of wavelength (Fig. 8).

One could see that the nearly phase-matched mid-IR radiation generation is possible in an extremely broad spectral range (at least from 2 to 14 μm). More specifically, within this spectral range the wavevector mismatch ΔK is less than 0.15 cm^{-1}. Therefore, the minimal coherence length could exceed 22 cm. This means that, as was tested experimentally, efficient mid-infrared radiation generation in air is possible using pump focusing lenses of long focal length. It is worth noting that, in principle, apart from the already demonstrated wide tunability of mid-IR radiation, ultrabroadband mid-IR pulses can also be generated using this process. Also, since the generated mid-IR beams have low divergence and high spatial quality, they can be used directly for various spectroscopic applications and as a seed for more powerful laser systems. In addition, we believe that this process can also be used for generation and direct amplification of ultrabroadband few-cycle mid-IR pulses if broadband pump pulses are applied.

Gaseous media, such as ambient air or laser-created air plasma, have some advantages over nonlinear optical crystals, including low optical dispersion, wide optical transparency, and a high optical damage threshold. Since the volume of nonlinear interaction in gases can be large, four-wave mixing is suitable for high-power applications using large femtosecond laser systems. However, the nonlinearity of gaseous media is usually smaller than that of nonlinear crystals, suggesting lower conversion efficiency, which, however, can be substantially increased by applying higher input laser intensities. Another disadvantage of gaseous media irradiated by intense laser beams is their tendency to self-focus and split into multiple plasma filaments, which can distort the phase-matching conditions and the spatial output beam parameters. This problem can be solved using cylindrical laser beam focusing, which, at high pump powers, can help avoid plasma-induced laser defocusing by creating a two-dimensional air plasma sheet (Kuk et al. 2016).

In conclusion, we demonstrated and analyzed four-wave mixing in air using loosely focused femtosecond bichromatic laser pulses. The results of the proof-of-principle experiment show that this process can produce well-collimated mid-infrared beams within a wide

wavelength range, from at least 2 to 12 μm. Apart from its potential applications in high-power laser systems, this method could be considered for various spectroscopic applications requiring high-quality mid-infrared pulses.

Acknowledgements The authors acknowledge the use of the ELI Beamlines Facility, Extreme Light Infrastructure ERIC. V. Vaičaitis, S. Espinoza, and M. Rebarz thank Jakob Andreasson for support.

Author contributions Conceptualization and design: Virgilijus Vaičaitis. Data collection: Virgilijus Vaičaitis, Mateusz Rebarz, and Shirly Espinoza. Formal analysis: Virgilijus Vaičaitis and Ona Balachninaitė. Writing–original draft: Virgilijus Vaičaitis. Writing–review and editing: all authors. All authors read and approved the final manuscript.

Funding Open access publishing supported by the institutions participating in the CzechELib Transformative Agreement. This research has been carried out in the framework of the "Universities' Excellence Initiative" programme by the Ministry of Education, Science and Sports of the Republic of Lithuania under the agreement with the Research Council of Lithuania (project No. S-A-UEI-23-6).

Data availability The datasets generated and analyzed during the current study are available from the corresponding author on reasonable request.

Declarations

Conflict of interest The authors declare no conflict of interest.

Open Access This article is licensed under a Creative Commons Attribution 4.0 International License, which permits use, sharing, adaptation, distribution and reproduction in any medium or format, as long as you give appropriate credit to the original author(s) and the source, provide a link to the Creative Commons licence, and indicate if changes were made. The images or other third party material in this article are included in the article's Creative Commons licence, unless indicated otherwise in a credit line to the material. If material is not included in the article's Creative Commons licence and your intended use is not permitted by statutory regulation or exceeds the permitted use, you will need to obtain permission directly from the copyright holder. To view a copy of this licence, visit http://creativecommons.org/licenses/by/4.0/.

References

Aközbek, N., Iwasaki, A., Becker, A., Scalora, M., Chin, S.L., Bowden, C.M.: Third-harmonic generation and self-channeling in air using high-power femtosecond laser pulses. Phys. Rev. Lett. **89**, 143901 (2002). https://doi.org/10.1103/PhysRevLett.89.143901

Boyd, R.W.: Nonlinear Optics, 2nd edn. Academic Press, San Diego, CA (2003)

Brabec, T., Krausz, F.: Intense few-cycle laser fields: frontiers of nonlinear optics. Rev. Mod. Phys. **72**, 545–591 (2000). https://doi.org/10.1103/RevModPhys.72.545

Calabrese, L.S.C., Stingel, A.M., Petersen, P.B.: Ultrafast continuum mid-infrared spectroscopy: probing the entire vibrational spectrum in a single laser shot with femtosecond time resolution. Opt. Lett. **37**(12), 2265–2267 (2012). https://doi.org/10.1364/OL.37.002265

Ciddor, P.E.: Refractive index of air: new equations for the visible and near infrared. Appl. Opt. **35**, 1566–1573 (1996). https://doi.org/10.1364/AO.35.001566

Clerici, M., Peccianti, M., Schmidt, B.E., Caspani, L., Shalaby, M., Giguère, M., Lotti, A., Couairon, A., Légaré, F., Ozaki, T., Faccio, D., Morandotti, R.: Wavelength scaling of terahertz generation by gas ionization. Phys. Rev. Lett. **110**, 253901 (2013). https://doi.org/10.1103/PhysRevLett.110.253901

Dietze, D., Darmo, J., Roither, S., Pugzlys, A., Heyman, J.N., Unterrainer, K.: Polarization of terahertz radiation from laser generated plasma filaments. J. Opt. Soc. Am. B **26**, 2016–2027 (2009). https://doi.org/10.1364/JOSAB.26.002016

Dubietis, A., Matijošius, A.: Table-top optical parametric chirped pulse amplifiers: past and present. Opto-Electr. Adv. **6**, 220046 (2023). https://doi.org/10.29026/oea.2023.220046

Fuji, T., Suzuki, T.: Generation of sub-two-cycle mid-infrared pulses by four-wave mixing through filamentation in air. Opt. Lett. **32**, 3330–3332 (2007). https://doi.org/10.1364/OL.32.003330

Gaižauskas, E., Pentaris, D., Efthimiopoulos, T., Vaičaitis, V.: Probing electronic coherences by combined two- and one-photon excitation in atomic vapors. Opt. Lett. **38**, 124–126 (2013). https://doi.org/10.1364/OL.38.000124

Gaižauskas, E., Steponkevičius, K., Vaičaitis, V.: Fifth-order intensity autocorrelations based on six-wave mixing of femtosecond laser pulses. Phys. Rev. A **93**, 023813 (2016). https://doi.org/10.1103/PhysRevA.93.023813

Israelsen, N.M., Petersen, C.R., Barh, A., et al.: Real-time high-resolution mid-infrared optical coherence tomography. Light Sci. Appl. **8**(1), 11 (2019). https://doi.org/10.1038/s41377-019-0122-5

Jang, D., Schwartz, R.M., Woodbury, D., Griff-McMahon, J., Younis, A.H., Milchberg, H.M., Kim, K.Y.: Efficient terahertz and Brunel harmonic generation from air plasma via mid-infrared coherent control. Optica **6**, 1338–1341 (2019). https://doi.org/10.1364/OPTICA.6.001338

Jean, B., Bende, T.: Mid-IR laser applications in medicine. In Sorokina, I.T., Vodopyanov, K.L.: editors, Solid-State Mid-Infrared Laser Sources, volume 89 of Topics in Applied Physics. Springer, Berlin, Heidelberg, (2003). https://doi.org/10.1007/3-540-36491-9_11

Khosrofian, J.M., Garetz, B.A.: Measurement of a Gaussian laser beam diameter through the direct inversion of knife-edge data. Appl. Opt. **22**, 3406–3410 (1983). https://doi.org/10.1364/AO.22.003406

Kim, K.Y., Taylor, A.J., Glownia, J.H., Rodriguez, G.: Coherent control of terahertz supercontinuum generation in ultrafast laser-gas interactions. Nat. Photonics **2**, 605–609 (2008). https://doi.org/10.1038/nphoton.2008.153

Kuk, D., Yoo, Y.J., Rosenthal, E.W., Jhajj, N., Milchberg, H.M., Kim, K.Y.: Generation of scalable terahertz radiation from cylindrically focused two-color laser pulses in air. Appl. Phys. Lett. **108**, 121106 (2016). https://doi.org/10.1063/1.4944843

Li, J., Lu, J., Chew, A., Han, S., Li, J., Wu, Y., Wang, H., Ghimire, S., Chang, Z.: Attosecond science based on high harmonic generation from gases and solids. Nat. Commun. **11**, 2748 (2020). https://doi.org/10.1038/s41467-020-16480-6

Liu, K., Liu, J., Shi, H., Tan, F., Wang, P.: High power mid-infrared supercontinuum generation in a single-mode ZBLAN fiber with up to 21.8 W average output power. Opt. Express **22**, 24384 (2014). https://doi.org/10.1364/OE.22.024384

Lukin, M.D., Hemmer, P.R., Scully, M.O.: Resonant nonlinear optics in phase-coherent media. In Bederson, B., Walther, H.: editors, Advances in Atomic, Molecular, and Optical Physics, volume 42, pages 347–386. Academic Press, (2000)

Ma, J., Qin, Z., Xie, G., Qian, L., Tang, D.: Review of mid-infrared mode-locked laser sources in the 2.0–3.5 μm spectral region. Appl. Phys. Rev. **6**, 021317 (2019). https://doi.org/10.1063/1.5037274

Mathar, R.J.: Refractive index of humid air in the infrared: model fits. J. Opt. A: Pure Appl. Opt. **9**, 470–476 (2007). https://doi.org/10.1088/1464-4258/9/5/008

Mirov, S., Moskalev, I., Vasilyev, S., Smolski, V., Fedorov, V., Martyshkin, D., Peppers, J., Mirov, M., Dergachev, A., Gapontsev, V.: Frontiers of mid-ir lasers based on transition metal doped chalcogenides. IEEE J. Sel. Top. Quantum Electron. **24**, 1601829 (2018). https://doi.org/10.1109/JSTQE.2018.2808284

Penzkofer, A., Lehmeier, H.J.: Theoretical investigation of noncollinear phase-matched parametric four-photon amplification of ultrashort light pulses in isotropic media. Opt. Quantum Electron. **25**, 815–844 (1993). https://doi.org/10.1007/BF00430189

Steinle, T., Mörz, F., Steinmann, A., Giessen, H.: Ultra-stable high average power femtosecond laser system tunable from 1.33 to 20 μm. Opt. Lett. **41**, 4863–4866 (2016). https://doi.org/10.1364/OL.41.004863

Tamulienė, V., Juškevičiūtė, G., Buožius, D., Vaičaitis, V., Morgner, U., Babushkin, I.: Influence of tunnel ionization to third-harmonic generation of infrared femtosecond laser pulses in air. Sci. Rep. **10**, 17437 (2020). https://doi.org/10.1038/s41598-020-74263-x

Théberge, F., Aközbek, N., Liu, W., Becker, A., Chin, S.L.: Tunable ultrashort laser pulses generated through filamentation in gases. Phys. Rev. Lett. **97**, 023904 (2006). https://doi.org/10.1103/PhysRevLett.97.023904

Vaičaitis, V.: Cherenkov-type phase-matched third harmonic generation in air. Optics Commun. **185**, 197–202 (2000). https://doi.org/10.1016/S0030-4018(00)00997-4

Vaičaitis, V., Ivanov, M., Adomavicius, K., Svirskas, Ž., Morgner, U., Babushkin, I.: Influence of laser-preformed plasma on THz wave generation in air by bichromatic laser pulses. Laser Phys. **28**, 095402 (2018). https://doi.org/10.1088/1555-6611/aaca5f

Vaičaitis, V., Butkus, R., Balachninaitė, O., Morgner, U., Babushkin, I.: Diffraction-enhanced femtosecond white-light filaments in air. Appl. Phys. B **124**, 221 (2018). https://doi.org/10.1007/s00340-018-7090-y

Vaičaitis, V., Balachninaitė, O., Matijošius, A., Babushkin, I., Morgner, U.: Direct time-resolved plasma characterization with broadband terahertz light pulses. Phys. Rev. E **107**, 015201 (2023). https://doi.org/10.1103/PhysRevE.107.015201

Werner, K., Gruzdev, V., Talisa, N., Breusing, N., Kuehn, W., Woerner, M., Elsaesser, T.: Single-shot multi-stage damage and ablation of silicon by femtosecond mid-infrared laser pulses. Sci. Rep. **9**, 19993 (2019). https://doi.org/10.1038/s41598-019-56384-0

Wilson, D.J., Summers, A.M., Zigo, S., Davis, B., Robatjazi, S.-J., Powell, J.A., Rolles, D., Rudenko, A., Trallero-Herrero, C.A.: An intense, few-cycle source in the long-wave infrared. Sci. Rep. **9**, 6002 (2019). https://doi.org/10.1038/s41598-019-42433-1

Yao, Y., Hoffman, A.J., Gmachl, C.: Mid-infrared quantum cascade lasers. Nat. Photonics **6**, 432 (2012). https://doi.org/10.1038/nphoton.2012.143

Yu, Y., Gai, X., Wang, T., Ma, P., Wang, R., Yang, Z., Choi, D.-Y., Madden, S., Luther-Davies, B.: Mid-infrared supercontinuum generation in chalcogenides. Opt. Mater. Exp. **3**, 1075 (2013). https://doi.org/10.1364/OME.3.001075

Publisher's Note Springer Nature remains neutral with regard to jurisdictional claims in published maps and institutional affiliations.